Applied Surface Science 457 (2018) 856–862

Contents lists available at ScienceDirect

Applied Surface Science

journal homepage: www.elsevier.com/locate/apsusc

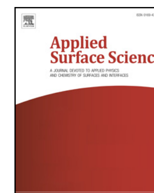

Full Length Article

Comparative study of Ti and Cr adhesion to the AlN ceramic: Experiments and calculations

Shanshan Zhang[a], Weichao Jin[a], Huisheng Yang[a], Kewei Gao[a], Xiaolu Pang[a,*], Luchun Yan[a], Alex A. Volinsky[b]

[a] *Department of Materials Physics and Chemistry, University of Science and Technology Beijing, Beijing 100083, China*
[b] *Department of Mechanical Engineering, University of South Florida, Tampa, FL 33620, USA*

ARTICLE INFO

Keywords:
Adhesion
Thin film
Interface
Ti, Cr
AlN substrate
First principles

ABSTRACT

In this manuscript, ceramic substrates with different adhesion layers were prepared by the direct-plated-copper (DPC) method. Microstructure and mechanical properties were investigated by scanning electron microscopy (SEM) and adhesion strength tests. SEM results showed that the AlN/Ti/Cu interface had fewer defects than AlN/Cr/Cu and AlN/Cu. The adhesion strength of the Ti layer samples was about 16.5 MPa, which is much higher compared with Cr and no adhesion layer samples. The adhesion strength of the AlN/Ti/Cu sample was the highest, followed by AlN/Cr/Cu, and AlN/Cu adhesion was the lowest. The AlN (0 0 1)/Ti (0 0 1) and AlN (0 0 1)/Cr (1 1 0) interfaces were studied by the first principles calculations based on the density functional theory (DFT). It appears that the Ti—N bonds were formed by the Ti-spd and N-p orbital hybridization. Moreover, the electron transition from Ti atom to N atom was higher than that from Cr to N. The bond length of Ti—N bond is shorter than Cr—N bond length, and its population has proven that Ti—N has stronger covalent character, which may be the reason why the AlN/Ti/Cu interface has higher interfacial stability than AlN/Cr/Cu.

1. Introduction

Direct-plated-copper (DPC) is a method of ceramic metallization, which can provide an alternative to conventional substrates for better heat dissipation in high power module applications [1]. DPC can provide thin film metallization of ceramic substrates with high precision and surface smoothness. Compared with other ceramic metallization methods [2], DPC has lower metallization temperature of about 300 °C. Direct-bonded-ceramic (DBC) refers to a metallization method in which copper and ceramics are bonded together by eutectic reactions, but the operating temperature is about 1065–1085 °C. Due to the high operating temperature, the interface is prone to defects generation, resulting in degraded thermal cycling performance. In comparison, direct-plated-copper method operates at a lower temperature, and the process is easier to control [3,4]. Aluminum nitride (AlN) is a promising ceramic substrate material with the thermal expansion coefficient of about $4.5 \times 10^{-6}\ K^{-1}$, which is quite different compared with most metals. Furthermore, AlN is a strong covalent compound, which has certain difficulties with metallization [5,6]. It has been reported that most metals have poor wettability with AlN [7–12]. Ceramics and metals have significant differences in physical and chemical properties, thus efforts have been made to find better methods to bond metals and ceramics materials.

Stronger chemical bonds formed between ceramics and metals result in better adhesion, which also determines the quality and reliability of the products to a large extent. Thus, it's crucial to form stronger solid bonds between ceramics and metals. Some of the elements can form high-lattice-based compounds with N, which are often selected as adhesion layers [13,14]. In some literature reports, Cr and Ti are often used as the adhesion layer for DPC [15–17]. In this research, Cr and Ti are compared using experiments and calculations to identify which material is more suitable for the adhesion layer. In recent years the first principles methods based on the density functional theory (DFT) have been utilized to investigate interfacial properties [18]. Some research papers reported that the combination of ceramics and metals depends on the lattice mismatch between them, i.e., the smaller the mismatch, the higher the bond strength [19].

In this work, titanium and chromium were selected as transition layer metals, which were deposited by magnetron sputtering on the substrate surface as the first layer. Experiments and theoretical predictions were used to illustrate the essence of the interfaces. We focused on the calculation of the interfacial free energy of metal/ceramic interfaces combined with the adhesion strength tests and scanning electron microscopy (SEM) characterization. The work of separation,

* Corresponding author.
E-mail address: pangxl@mater.ustb.edu.cn (X. Pang).

https://doi.org/10.1016/j.apsusc.2018.07.023
Received 18 December 2017; Received in revised form 29 June 2018; Accepted 3 July 2018
Available online 04 July 2018
0169-4332/ © 2018 Elsevier B.V. All rights reserved.

Table 1
Parameters of multi-arc ion sputtering.

	Cr film	Ti film	Cu film
Power current: I, A	150	150	300
Working gas: Ar (99.99%) Pressure, Torr	3×10^{-3}	3×10^{-3}	3×10^{-3}
Sputtering time: t, min	5	5	90

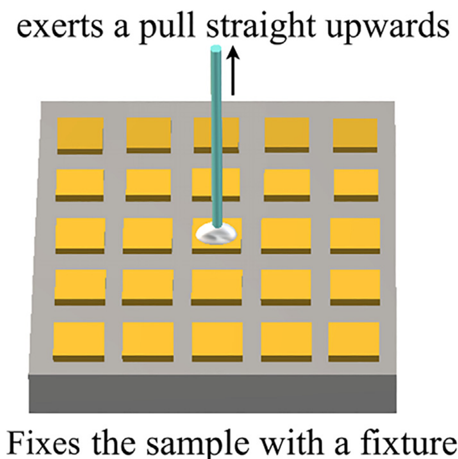

Fig. 1. Method of adhesion strength test.

$W_{AlN/M}^{hkl/h'k'l'}$, was used to measure the interface bond strength.

2. Experiments

2.1. Materials and methods

Ceramic substrates were manufactured by the DPC method. AlN ceramics substrates were 0.635 mm thick, containing Y_2O_3. Then atomic level cleaning of the surface of the aluminum nitride ceramic was performed prior to sputtering. AlN substrates were multi-arc ion treated prior to sputtering. The sputtering temperature varied from 423 K to 473 K. The thickness of the Ti and Cr adhesion layers was 20–200 nm. Then 6 µm copper seed layer was sputtered on top of adhesion layers. The deposition process parameters were optimized, as listed in Table 1. Cr, Ti and Cu targets were 99.99% pure.

Cu electroplating was performed for about 60 min to thicken the metallization layer with 2 A/dm^2 current power. The final Cu layer thickness was about 20 µm. The cross-section morphology was observed by field emission scanning electron microscope (ZEISS SUPRA 55, Germany) with 5 kV operating voltage. In order to characterize the adhesion strength between metal and ceramics, slow tensile testing machine was used. As shown in Fig. 1, samples for adhesion strength test were etched into 5 × 5 mm^2 arrays, then fixed the sample with a fixture and exerted a pull straight upwards by slow tensile testing machine until the metal and the ceramic layers were separated.

2.2. Results

Cross-section morphology of the AlN/Cu, AlN/Ti/Cu and AlN/Cr/Cu interfaces is shown in Fig. 2. The samples were broken by a glass knife. There are cracks at the AlN/Cu and AlN/Cr/Cu interfaces, suggesting that the interfacial bond strength is low. The crack throughout the AlN/Cu interface is shown in Fig. 2(a). Cr adhesion layer improved interfacial bonding, but there are still some cracks at the interface, as seen in Fig. 2(b). The metal layer is not completely detached from the ceramics, and there are still adhered parts between the metal and ceramics. However, in Fig. 2(c), where Ti is an adhesion layer, the cross-section morphology shows no defects, such as cracks or pores. Since the cross sections of the samples were made in the same way, the metal layer was peeled off the substrate to prove that the bond strength is poor. This test proved that titanium and chromium can improve ceramic/metal interfacial adhesion.

EDS results of the AlN/Ti/Cu interface are shown in Fig. 3. Ti content has a gradient change from the AlN side to the Cu side. As shown in Fig. 3(d) and (e), the interface has titanium and nitrogen, and

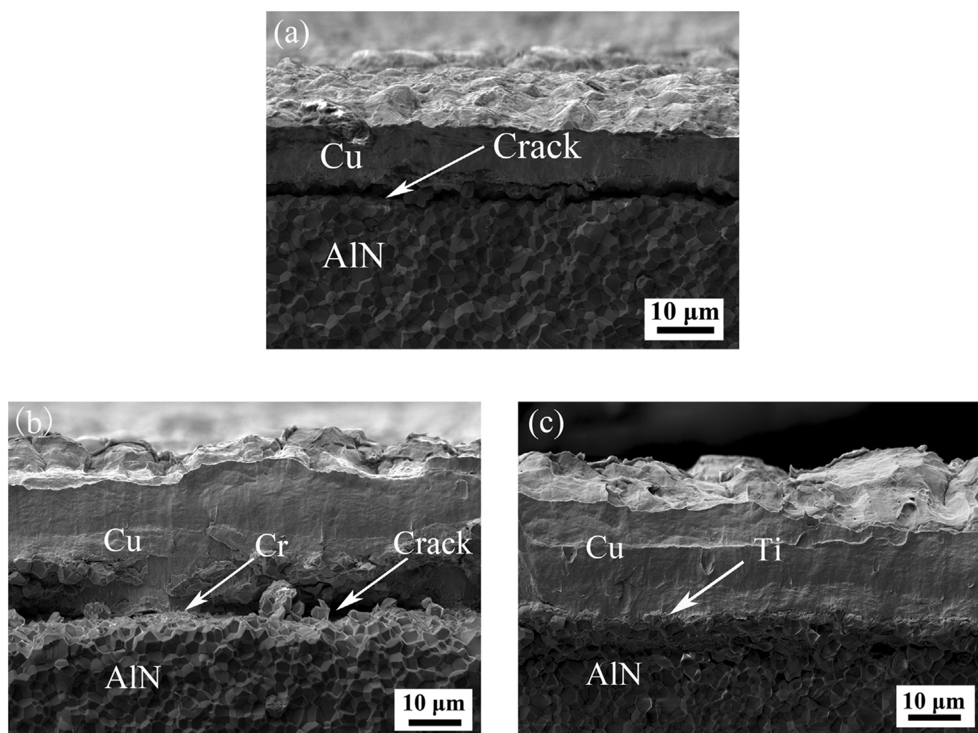

Fig. 2. Cross section morphology of different transition layers on ceramic substrate: (a) AlN/Cu; (b) AlN/Cr/Cu and (c) AlN/Ti/Cu.

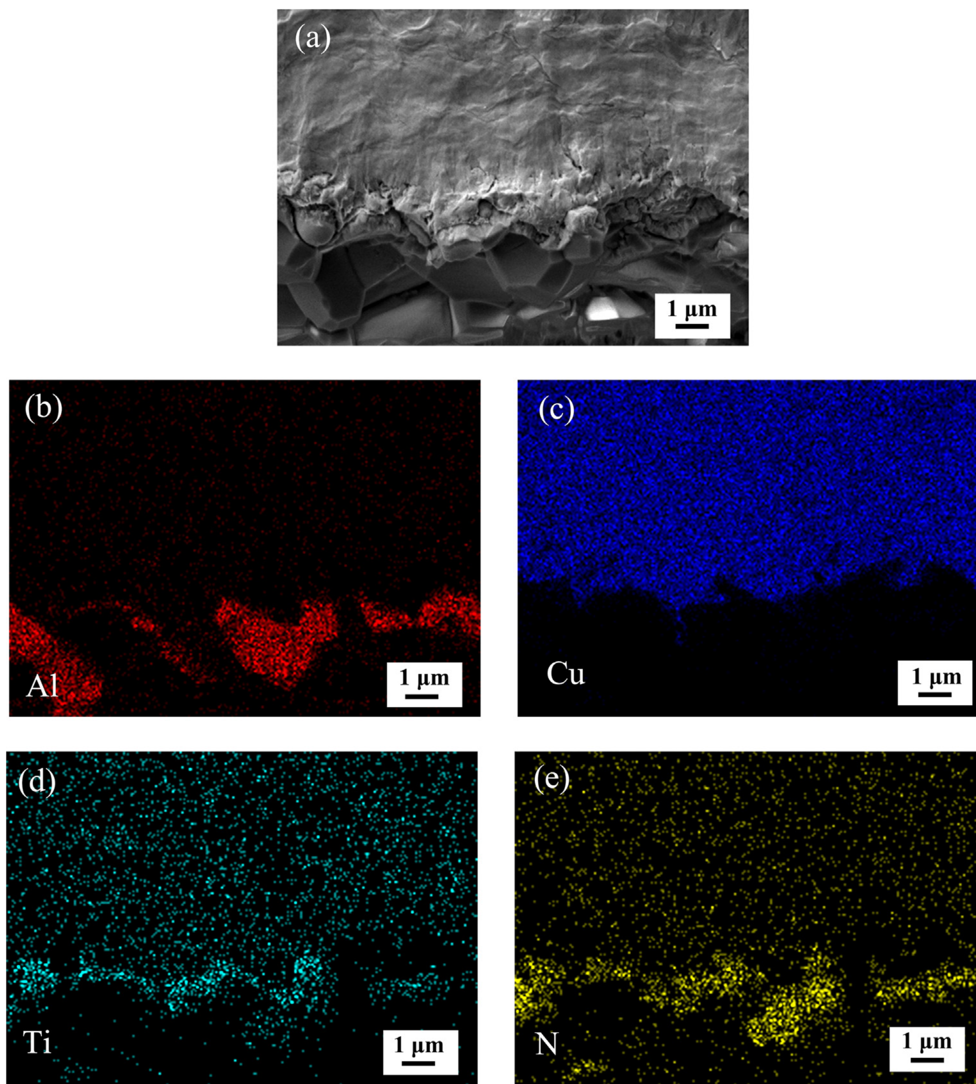

Fig. 3. Element area distribution of diffusion at the AlN/Ti/Cu interface. Cross section morphology of: (a) AlN/Ti/Cu; (b) Al; (c) Cu; (d) Ti and (e) N.

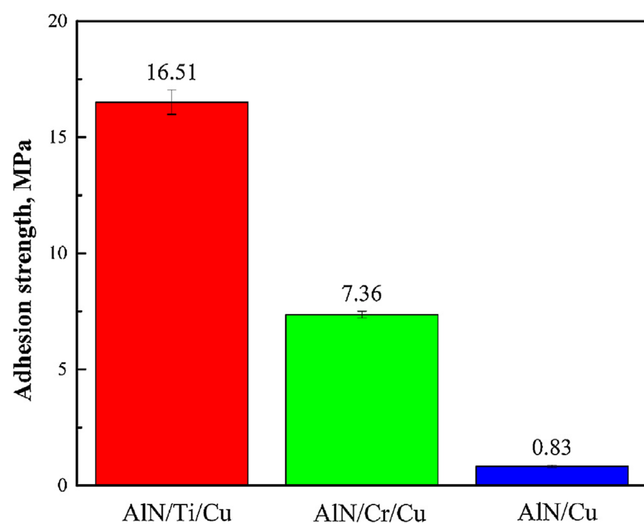

Fig. 4. Adhesion strength of AlN/Cu, AlN/Ti/Cu and AlN/Cr/Cu electroplated for 60 min.

the thickness of the interface reaction layer is about 1–3 μm. It can also be observed that some of Ti diffused into copper.

Fig. 4 shows the results of adhesion test for the three kinds of samples, AlN/Cu, AlN/Ti/Cu and AlN/Cr/Cu. The adhesion strength of AlN/Ti/Cu has been greatly improved compared with the other two samples. The adhesion strength in descending order is AlN/Ti/Cu > AlN/Cr/Cu > AlN/Cu. The adhesion strength with titanium as an adhesion layer is about 16.5 MPa. The adhesion strength of the samples with no adhesion layers is far less than the samples with adhesion layers.

3. Theoretical calculations

3.1. Calculation methods and models

In this research, the works of separation at AlN (0 0 1)/Ti (0 0 1) and AlN (0 0 1)/Cr (1 1 0) interfaces was calculated using the first principles Cambridge serial total energy package (CASTEP). The calculations employed the generalized Perdew, Burke, and Ernze (GGA-PBE) gradient approximation for the exchange–correlation function [19,20]. The irreducible wedge of the Brillouin zone was integrated by means of the Monkhorst-Pack scheme [21] using the 9 × 9 × 9 grid. The surfaces and interfaces were modeled using the supercell approach with periodic boundary conditions. The convergence parameters were set as follows.

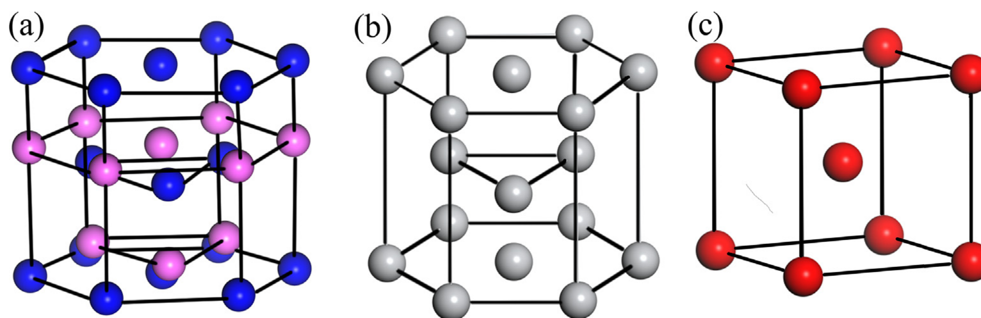

Fig. 5. Crystal structures of: (a) AlN; (b) Ti and (c) Cr.

Table 2
Information of the models.

Parameter name	Parameter value	Select reason
Number of surface layer	Ti: 9 layers AlN: 10 layers Cr: 6 layers	Convergence test
Crystal orientation	(1 × 1) AlN (0 0 1)/ (1 × 1) Ti (0 0 1) $(2\sqrt{3} \times 2\sqrt{3})$ AlN (0 0 1)/(4 × 4) Cr (1 1 0)	Close-packed plane Lattice mismatch
Converged criterion (surface)	1 meV/surface unit cell	
Interface area	AlN (0 0 1)/Ti (0 0 1): 15.96 $Å^2$ AlN (0 0 1)/Cr (1 1 0): 92.59 $Å^2$	
Lattice parameter	Calculated value: Ti: a = b = 2.941 Å, c = 4.663 Å Cr: a = b = c = 2.794 Å AlN: a = b = 3.126 Å, c = 5.008 Å	Experimental value: Ti: a = b = 2.951 Å, c = 4.679 Å [26] Cr: a = b = c = 2.884 Å [27] AlN: a = b = 3.110 Å, c = 4.980 Å [28]

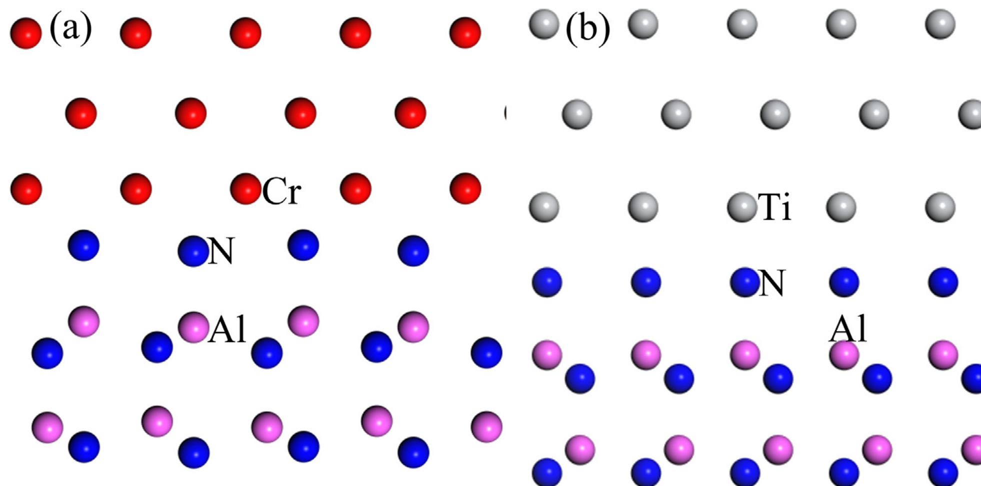

Fig. 6. Simulated structures of: (a) AlN (0 0 1)/Ti (0 0 1) and (b) AlN (0 0 1)/Cr(1 1 0) interfaces. Green balls represent Ti atoms, while the purple and blue balls represent aluminum and nitrogen atoms, respectively. Gray balls stand for Cr.

Table 3
The work of separation of the AlN/M interfaces.

	$E^{hkl}_{surf\,(M)}$, eV	$E^{hkl}_{surf\,(AlN)}$, eV	$E^{001/001}_{AlN/M}$, eV	$W^{001/001}_{AlN/M}$, J/m^2
AlN(0 0 1)/Cr (1 1 0)	−221988.755	−23732.831	−245780.915	1.454
AlN(0 0 1)/Ti (0 0 1)	−9616.887	−1978.793	−11598.455	4.838

Note: the lattice constant is the standard value for pure bulk materials.

The plane-wave cut-off energy was selected as 400 eV for all calculations, which was sufficient to obtain reliable results. Other parameters were set with high precision. For the geometry optimization, all theatoms in the supercell were fully relaxed until the energy convergence of 5e − 6 eV/atom, and the thick vacuum layer was 18 Å. In this case the Brillouin zone was using the 9 × 9 × 1 grid. To research the ceramic/metal interface, it is significant to make sure the two slabs were thick enough to show the bulk-like character [22]. If the slabs are too thin, material properties could not be characterized, while in contrast, thick slabs would increase calculation time. Therefore, appropriate slab thickness was crucial for calculations. The minimum slabs thickness was obtained by calculating the convergent properties of the surface energy. The AlN surface energy ranging from 6 to 14 layers was calculated until the energy was converged by using the following formula [23]:

$$E^{hkl}_{surf} = \frac{E^{hkl}_{surf} - \frac{N^{hkl}_{slab}}{N_{bulk}} E_{bulk}}{2A^{hkl}} \quad (1)$$

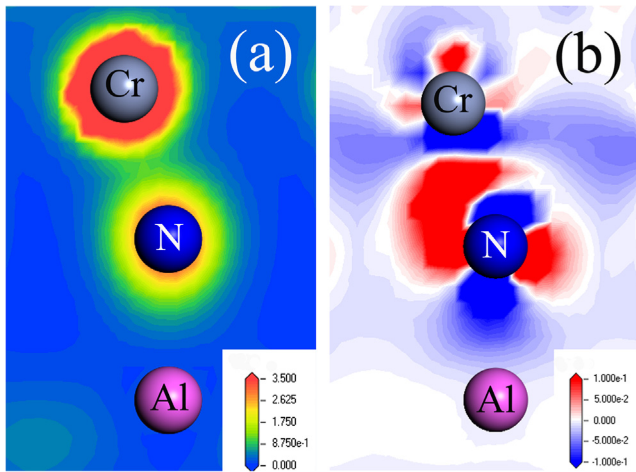

Fig. 7. (a) Electron density and (b) electron density difference along the (0 1 0) plane of AlN (0 0 1)/Cr (1 1 0) interface.

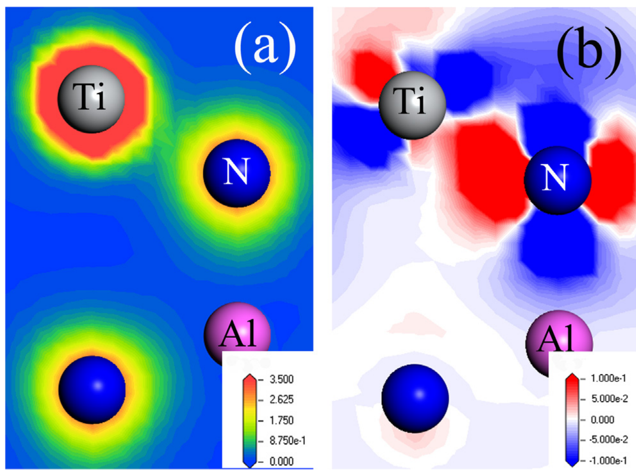

Fig. 8. (a) Electron density and (b) electron density difference along the (1 1 0) plane of AlN (0 0 1)/Ti (0 0 1) interface.

Here, E_{slab}^{hkl}, N_{slab}^{hkl}, E_{bulk}, and N_{bulk}represent the total energy of (*hkl*) surfaces and the number of atoms in the slab and the bulk. Al-terminated model was chosen to build the interfaces, and all atoms were relaxed in all directions. The minimum number of layers was determined by the convergence test. The work of separation ($W_{AlN/M}^{001/hkl}$) can characterize the adhesion strength of the interface. It is commonly used to define the energy per unit area required to separate the two parts of an interface and to form two infinitely separated free surfaces [23]:

$$W_{AlN}^{001/hkl} = \frac{E_{surf\,(AlN)}^{001} + E_{surf\,(M)}^{hkl} - E_{AlN/M}^{001/hkl}}{A_{AAN/M}^{001/hkl}} \tag{2}$$

The letter M refers to one metal, $E_{surf\,(AlN)}^{001}$ and $E_{surf\,(M)}^{hkl}$ represent the total energy of the surface structure, $E_{AlN/M}^{001/hkl}$ is the total energy of the interface structure formed by the AlN (0 0 1) and M (*hkl*), and $A_{AlN/M}^{001/hkl}$ is the corresponding interface area.

Various crystal orientations of the surface determine different work of separation. In general, the close-packed plane is the most stable and has the lowest surface energy. Both AlN and Ti have hexagonal close packed (hcp) structure, and their lattice constants are close to each other, while Cr has body-centered cubic (bbc) structure, as shown in Fig. 5.

Due to the difference in crystal structure and lattice constant, there must be lattice mismatch when modeling the interface. Therefore, appropriate rotation and resizing of the lattices were applied to reduce the mismatch. we intentionally selected interfaces having lattice mismatch roughly less than 5% [24,25]. Periodicity is introduced in the direction parallel to the interface to obtain the interface with small mismatch. $(2\sqrt{3} \times 2\sqrt{3})$ AlN (0 0 1) cell and (4 × 4) Cr (1 1 0) cell are adopted to build the AlN (0 0 1)/Cr (1 1 0) interface. The total number of atoms of the model is about 216, and the mismatch of the interface is about 4.7%. For AlN and Ti, they are both hcp structure, and the lattice parameters of the two are relatively close (Ti: a = b = 2.941 Å, c = 4.663 Å, AlN: a = b = 3.126 Å, c = 5.008 Å). For this interface with less mismatch, the mean value of the lattice parameters of the two surfaces is considered for adoption. When (1 × 1) AlN (0 0 1)/(1 × 1) Ti (0 0 1) is established in this way, one surface is stretched and the other is compressed, about 3.1% mismatch is generated. The total number of atoms in the model is 29. We pointed out that smaller lattice mismatches may be obtained, but considering the calculation quantity and economy, these models can meet the demand of calculation precision.

Information of the models are shown in Table 2, and the lattice parameter of calculated value is close to the experimental value indicating that the calculated data is reliable. The models of the AlN (0 0 1)/Ti (0 0 1) and AlN (0 0 1)/Cr (1 1 0) interfaces are shown in Fig. 6.

3.2. Work of separation

The work of separation, $W_{AlN/M}^{001/hkl}$, is listed in Table 3. The AlN (0 0 1)/Cr (1 1 0) interface work of separation is 1.454 J/m^2, while the

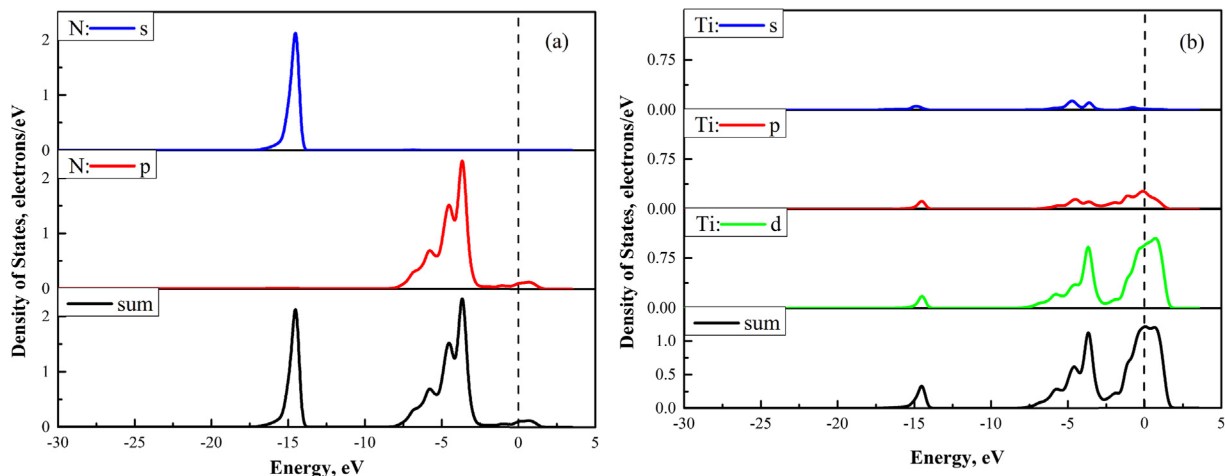

Fig. 9. Density of states (DOS) for the relaxed AlN/Cr interface: (a) N and (b) Cr.

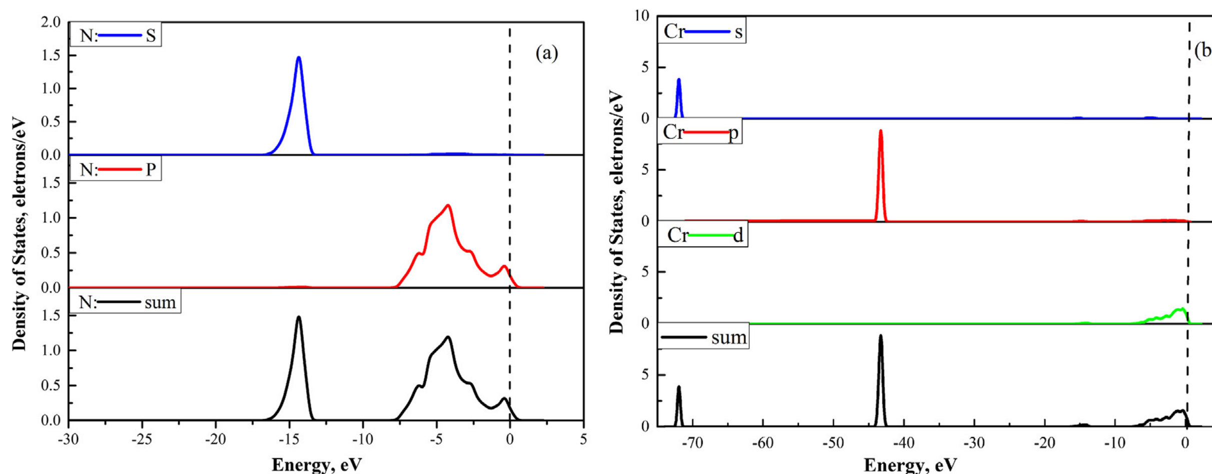

Fig. 10. Density of states (DOS) for the relaxed AlN/Ti interface: (a) N and (b) Ti.

Table 4
The population value and bond length of Ti—N and Cr—N at the interface.

	Species	S	P	d	Total	Charge, e
AlN/Ti	N	1.70	4.17	0	5.87	−0.87
	Ti	2.26	6.65	2.51	11.42	0.58
	Ti_{Bulk}	2.39	6.96	2.69	12.00	0
	Bond		Population		Length	
	N—Ti		1.39		1.95	
AlN/Cr	N	1.72	3.93	0	5.65	−0.65
	Cr	2.24	6.65	4.87	13.76	0.24
	Cr_{Bulk}	2.1	6.92	4.99	14.00	0
	Bond		Population		Length	
	N—Cr		0.27		2.1	

AlN (0 0 1)/Ti (0 0 1) interface work of separation is 4.838 J/m^2, which is obviously much higher, indicating that the AlN (0 0 1)/Ti (0 0 1) interface has larger work of separation. Titanium is a better choice for metallization of ceramics.

3.3. Electronic structures

The electron density (ED) and electron density difference (EDD) for AlN (0 0 1)/Cr (1 1 0) and AlN (0 0 1)/Ti (0 0 1) interfaces are presented in Figs. 7 and 8. The electron density difference $\Delta\rho$ was given by

$$\Delta\rho = \rho_{M/\mathrm{AlN}} - \rho_{\mathrm{AlN}} - \rho_M \quad (3)$$

where $\rho_{M/\mathrm{AlN}}$ is the total charge density of the interface systems, ρ_{AlN} and ρ_M are the isolated AlN slab and Ti slab of the same supercell, respectively. The letter M refers to one metal [29].

ED and EDD of AlN (0 0 1)/Cr (1 1 0) interface was along the (0 1 0) plane. And the ED and EDD of AlN (0 0 1)/Ti (0 0 1) interface was along the (1 1 0) plane. In Figs. 7(a) and 8(a), N atoms at the interface form a chemical bonding with the corresponding Ti or Cr atoms, and the electron accumulations between the two interfaces looks roughly the same.

Due to the different crystal structures of TiN and CrN, the atomic charge redistribution has different shapes in the EDD diagram. It can be seen from Figs. 7(b) and 8(b) that the electronic rearrangement of the two interfaces is confined to the two atomic layers near the interface, and the sublayers express the electronic characteristics of the body. In Figs. 7(b) and 8(b), the charge accumulation of N atom in the bonding direction of N-Ti and N-Cr should be observed, because some of the charge around N atoms comes from neighboring Al and N atoms. It can be seen that Ti has more charge transfer than Cr. Thus, Ti—N has more covalent bond properties than Cr—N and contributes more to interfacial bonding, and its structure is thermodynamically relatively stable.

3.4. Partial density of states

Figs. 9 and 10 show the partial density of states (PDOS) of AlN (0 0 1)/Cr (1 1 0) and AlN (0 0 1)/Ti (0 0 1). As shown in Fig. 9, Cr and N correspond to 0 eV through −6 eV, indicating that N and Cr are hybrid by Cr-3d and N-2p. The covalent bonds are formed at the interfaces of AlN (0 0 1)/Cr (1 1 0) due to the electron orbital hybridization. In Fig. 10 partial density of states (PDOS) of the atomic Ti and N near the interface has a corresponding relationship between −3 eV and −6 eV and at −14.5 eV. These corresponding peaks and their overlapping portions showed the hybridization between Ti-spd and N-sp. The p-orbital of the N-atom and the d-orbital of the Ti atom produce strong hybridization. In Figs. 9(a) and 10(a) the s-orbital of the N atom at −14.5 eV is very sharp and narrow, exhibiting strong localized characteristic. The s-orbital of N-atoms is also covalent with the adjacent Ti atoms in the vicinity of −14.5 eV. The state density passing through the Fermi surface is not zero, but is relatively small. The Ti—N bonds show properties of a certain metallic bond. Thus, the TiN bond has both covalent, ionic and metallic properties. These calculation results indicate that new bonds were formed between the adhesion layers and ceramic substrate at the interface. It can be justified that adhesion layers and aluminum nitride ceramics formed chemical bonds.

3.5. The Mulliken population analysis

The adhesion strength of the substrates is closely related to its chemical bond strength, and the chemical bonding is formed by orbitals of different overlapped atoms. In 1955 Mulliken [30] proposed to use the overlapping bond population to determine the molecular orbital bonding properties and interatomic chemical bonding strength. Mulliken distributes the charge in the atomic orbital overlapping region to the associated atomic orbital. The overlapping electron charge distributed between the two atoms is called overlapping bond population, and the number of electrons in the atomic space is the atomic charge population. In order to analyze the distribution and bonding of Ti—N and Cr—N in the system, atomic charge population and overlapping bond population were calculated, as shown in Table 4. Charge is evenly distributed in pure metal, and there is no charge transfer. So the charge transfer of Ti and Cr atoms at the interface is all used to bond with N atoms at the interface. It makes sense to compare the charge transfer of metal atoms at the interface. In the atomic charge population, it can be seen that the charge transfer amount of interface Ti in N-Ti is 0.58 e, which is higher than 0.24 e in N-Cr. The Ti—N overlapping bonding population is 1.39 e, while the Cr—N bond is 0.27 e. The smaller the overlapping population values, the smaller the number of common electrons between atoms. The strength of the covalent bonds formed

between the two atoms is also weaker. It can be seen from the population value that the covalent character of the Ti—N bond is greater than of the Cr—N bond. At the same time, the bond length of the TiN bond is 1.95 Å, which is shorter than the Cr—N bond length. The shorter the bond length, the stronger the bond strength.

4. Conclusions

In this paper, two transition layers for ceramic substrate preparation were compared. Two different 20–200 nm Ti and Cr adhesion layers were deposited on the surface of AlN substrates using multi-arc ion sputtering. The existence of the transition layer increases the interface bond strength. The sample with titanium had fewer cracks, and the adhesion strength of the AlN/Ti/Cu samples was about 16.5 MPa, which is higher than AlN/Cr/Cu and AlN/Ti/Cu samples. First principles calculations were used to study the AlN (0 0 1)/Ti (0 0 1) and AlN (0 0 1)/Cr (1 1 0) interfaces. The AlN (0 0 1)/Ti (0 0 1) work of separation is higher than AlN (0 0 1)/Cr (1 1 0). The simulation results were consistent with the experimental results. The Ti—N bond is formed by the Ti-spd and N-p orbital hybridization. The bond length of Ti—N bond is shorter than Cr—N bond length, and its population has proven that Ti—N has stronger covalent character. In conclusion, titanium metal is preferred as the transition layer in DPC ceramic substrate technology.

Acknowledgments

This work was supported by the Beijing Nova Program (Z171100001117075), the National Natural Science Foundation of China (51771025), and the Fundamental Research Funds for the Central Universities (FRF-TP-17-002C1).

References

[1] M.Y. Tsai, P.S. Huang, C.H. Lin, C.T. Wu, S.C. Hu, Mechanical design and analysis of direct-plated-copper aluminum nitride substrates for enhancing thermal reliability, Microelectron. Reliab. 55 (2015) 2589–2595.
[2] J. Reboun, J. Hlina, P. Totzauer, A. Hamacek, Effect of copper- and silver-based films on alumina substrate electrical properties, Ceram. Int. 44 (3) (2018) 3497–3500.
[3] J. Schulz-Harder, K. Exel, Advanced DBC (Direct Bonded Copper) substrates for high power and high voltage electronics, 22nd IEEE SEMI-THERM Symposium, 2006, pp. 230–231.
[4] J. Schulz-Harder, Advantages and new development of direct bonded copper substrates, Microelectron. Reliab. 43 (2003) 359–365.
[5] H.S. Hao, P. Fu, G. Li, S.H. Wang, Recent achievement in research for electronic packaging ceramic substrate materials, Ceramics 5 (2007) 24–27.
[6] S. Zhu, W. Wlosiński, Joining of AlN ceramic to metals using sputtered Al or Ti film, J. Mater. Process. Technol. 109 (2001) 277–282.
[7] W. Wang, W. Yang, Z. Liu, Y. Lin, S. Zhou, H. Qian, F. Gao, H. Yang, G. Li, Epitaxial growth of homogeneous single-crystalline AlN films on single-crystalline Cu(111) substrates, Appl. Surf. Sci. 294 (2014) 1–8.
[8] H. Yang, W. Wang, Z. Liu, W. Yang, G. Li, Epitaxial growth mechanism of pulsed laser deposited AlN films on Si(111) substrates, Cryst. Eng. Commun. 16 (2014) 3148–3154.
[9] C.Y. Su, C.T. Pan, M.S. Lo, Micro-structure and Mechanical Properties of AlN/Cu Brazed Joints, J. Mater. Eng. Perform. 23 (2014) 3299–3304.
[10] O.M. Akselsen, Review of diffusion bonding of ceramics, J. Mater. Sci. 27 (1992) 569–579.
[11] M.G. Nicholas, D.A. Mortimer, L.M. Jones, R.M. Crispin, Some observations on the wetting and bonding of nitride ceramics, J. Mater. Sci. 25 (1990) 2679–2689.
[12] N.Yu. Taranets, Y.V. Naidichi, Wettability of aluminum nitride by molten metals, Powder Metall. Met. Ceram. 35 (1996) 282–285.
[13] C. Chiu, C. Lin, Microstructural development of the AlN/Ti diffusion couple annealed at 1000 °C, J. Amer. Ceram. Soc. 4 (2008) 1273–1280.
[14] X.J. He, K. Tao, Y.D. Fan, Interfacial reactions of metal films with AlN substrates, Trans. Nonferrous Met. Soc. China 6 (1996) 81–85.
[15] T. Yasumoto, K. Yamakawa, N. Iwase, Reaction between AlN and metal thin films during high temperature annealing, J. Ceram. Soc. Jpn. 101 (1993) 944–948.
[16] X.B. Zhang, M.X. Chen, Z.L. Hao, S. Liu, Research on direct plated copper heat spreader and its thermal performances for high power LED packaging, International Conference on Electronic Packaging Technology, 2013, pp. 1193–1195.
[17] W.B. Carter, M.V. Papageorge, Titanium and tantalum coatings on aluminum nitride, J. Vac. Sci. Technol. A 10 (1992) 3460–3464.
[18] W.W. Xu, A.P. Horsfield, D. Wearing, P.D. Lee, First-principles calculation of Mg/MgO Interfacial Free Energies, J. Alloys Compd. 650 (2015) 228–238.
[19] Y. Tao, G.S. Ke, Y. Xie, Y.G. Chen, S. Shi, H. Guo, Adhesion strength and nucleation thermodynamics of four metals (Al, Cu, Ti, Zr) on AlN substrates, Appl. Surf. Sci. 357 (2015) 8–13.
[20] J.P. Perdew, A. Zunger, Self-interaction correction to density-functional approximations for many-electron systems, Phys. Rev. B 23 (1981) 5048–5079.
[21] H.J. Monkhorst, J.D. Pack, Simple points for Brillouin-zone integrations, Phys. Rev. B 13 (1976) 5188–5192.
[22] H.S. Abdelkader, H.I. Faraoun, First-principles Calculations of Adhesion, Bonding and Magnetism of the Fe/HfC Interface, J. Magn. Magn. Mater. 324 (2012) 4155–4160.
[23] X.G. Sun, K.W. Gao, X.L. Pang, H.S. Yang, A.A. Volinsky, Study on the growth mechanism and optical properties of sputtered lead selenide thin films, Appl. Surf. Sci. 356 (2015) 978–985.
[24] X.Y. Xu, H.Y. Wang, M. Zha, C. Wang, Z.Z. Yang, Q.C. Jiang, Effects of Ti, Si, Mg and Cu additions on interfacial properties and electronic structure of Al (111)/4H-SiC (0001) interface: a first-principles study, Appl. Surf. Sci. 437 (2018) 103–109.
[25] S.V. Dudiy, I. Bengt Lundqvist, First-principles density-functional study of metal-carbonitride interface adhesion: Co/TiC (001) and Co/TiN (001), Phys. Rev. B 64 (4) (2001) 045403.
[26] H. Schulz, K.H. Thiemann, Crystal structure refinement of AlN and GaN, Solid State Commun. 23 (1977) 815–819.
[27] A.Y. Kuksin, A.S. Rokhmanenkov, V.V. Stegailov, Atomic positions and diffusion paths of h and he in the α-Ti lattice, Phys. Solid State 55 (2013) 367–372.
[28] V.L. Moruzzi, P.M. Marcus, Antiferromagnetism in 3d transition metals, Phys. Rev. B. 42 (1990) 8361.
[29] L.M. Liu, S.Q. Wang, H.Q. Ye, Adhesion and bonding of the Al/TiC interface, Surf. Sci. 550 (2004) 46–56.
[30] R.S. Mulliken, Electronic population analysis on LCAO-MO molecular wave functions, J. Chem. Phys. 23 (1955) 1833–1840.